International Journal of Solids and Structures 51 (2014) 2460–2469

Contents lists available at ScienceDirect

International Journal of Solids and Structures

journal homepage: www.elsevier.com/locate/ijsolstr

A computational homogenization approach for the yield design of periodic thin plates. Part II : Upper bound yield design calculation of the homogenized structure

Jeremy Bleyer *, Patrick de Buhan

Université Paris-Est, Laboratoire Navier, Ecole des Ponts ParisTech-IFSTTAR-CNRS (UMR 8205), 6-8 av Blaise Pascal, Cité Descartes, 77455 Champs-sur-Marne, France

ARTICLE INFO

Article history:
Available online 29 March 2014

Keywords:
Yield design
Limit analysis
Periodic thin plates
Yield surface approximation
Second-order cone programming
Finite element method

ABSTRACT

In the first part of this work (Bleyer and de Buhan, 2014), the determination of the macroscopic strength criterion of periodic thin plates has been addressed by means of the yield design homogenization theory and its associated numerical procedures. The present paper aims at using such numerically computed homogenized strength criteria in order to evaluate limit load estimates of global plate structures. The yield line method being a common kinematic approach for the yield design of plates, which enables to obtain upper bound estimates quite efficiently, it is first shown that its extension to the case of complex strength criteria as those calculated from the homogenization method, necessitates the computation of a function depending on one single parameter. A simple analytical example on a reinforced rectangular plate illustrates the simplicity of the method. The case of numerical yield line method being also rapidly mentioned, a more refined finite element-based upper bound approach is also proposed, taking dissipation through curvature as well as angular jumps into account. In this case, an approximation procedure is proposed to treat the curvature term, based upon an algorithm approximating the original macroscopic strength criterion by a convex hull of ellipsoids. Numerical examples are presented to assess the efficiency of the different methods.

1. Introduction

In this joint work, the yield design of periodic thin plate structures is investigated. The first part of this work has been dedicated to the determination of the homogenized strength properties of different periodic plates through the numerical computation of a macroscopic strength criterion by means of finite elements and mathematical programming.

Homogenization theory in the framework of yield design (or limit analysis) of periodic structures has first been proposed in the work of Suquet (1985) and de Buhan (1986), where a proper definition of the macroscopic strength criterion involving the resolution of an auxiliary yield design problem formulated on the unit cell has been given. An analytical determination of the macroscopic strength criterion is very rare (e.g., the case of the multilayered soil under plane strain (de Buhan, 1986)) and often restricted to symmetric unit cell geometries and simple macroscopic loading (Maghous, 1991). Therefore, numerical methods are required, notably to conveniently capture the anisotropy of the homogenized material when preferential reinforcing directions are involved. The numerical resolution of the auxiliary problem can be tackled using incremental elasto-plastic approaches (Marigo et al., 1987) but a more natural method is to perform numerical limit analysis computations directly. This method, in conjunction with a finite element discretization, has been widely applied to different type of structures like porous media (Pastor and Turgeman, 1983; Turgeman and Pastor, 1987), periodic plates solicited in their own plane (Maghous, 1991; Francescato and Pastor, 1998), masonry walls (Sab, 2003), stone columns reinforced soils (Hassen et al., 2013) whereas the first part of this work (Bleyer and de Buhan, 2014) deals with thin periodic plates in bending.

Different numerical techniques have also been used to solve the corresponding optimization problem. In particular, linear programming (LP) associated to a piecewise linearization of the original local strength criterion has been very attractive due to the efficiency of interior point algorithms to solve LP problems. The extension of these algorithms to a wider class of convex programming problems, namely second-order cone programming (SOCP) enables today to solve limit analysis problems with their original nonlinear criterion very efficiently. SOCP has been notably used in the first part of this work to solve the static as well as the kinematic approach of the auxiliary problem.

* Corresponding author. Tel.: +33 (0)1 64 15 36 59.
E-mail address: jeremy.bleyer@enpc.fr (J. Bleyer).
URL: https://sites.google.com/site/bleyerjeremy/ (J. Bleyer).

http://dx.doi.org/10.1016/j.ijsolstr.2014.03.019
0020-7683/

Although an important amount of work has been dedicated to the numerical determination of macroscopic strength criteria of heterogeneous media, only a few papers, to the authors' knowledge, have been aimed at estimating the ultimate load of global structures made of such macroscopic strength criteria derived from the homogenization procedure. One can mention the work of Milani et al. (2006) concerning brick masonry or the following papers (Maghous et al., 1998; Hassen et al., 2013) on geotechnical problems. The small amount of work dedicated to this specific aspect is certainly due to the absence of closed-form expressions for the homogenized yield surfaces, which restrains their use to simple failure mechanisms for analytical applications. As regards numerical approaches, the homogenized yield surface has to be approximated, usually by piecewise linearization, to be dealt with. However, the number of hyperplanes describing the surface with a sufficient accuracy can be quite important, which is not desirable for efficient computations.

As regards the specific case of thin plates in bending, which is the scope of the present work, the strength criterion depends on the bending moment only. The yield line method, originally proposed by Johansen (1962), is an efficient upper bound kinematic method which considers only rigid mechanisms separated by yield lines where angular rotation discontinuities occur. Analytical upper bound estimates are, therefore, easily available and a numerical implementation using linear triangular finite element is also possible (Munro and Da Fonseca, 1978), although there are some inherent difficulties due to mesh dependency (Johnson, 1994; Jennings, 1996). However, to obtain tight upper bound estimates of plates in bending, dissipation through curvature has also to be taken into account. This requires to use a quadratic interpolation, at least, of the plate velocity field. Some authors proposed to use C^1-continuous high order finite elements to perform the upper bound approach (Capsoni and Corradi, 1999; Le et al., 2010) but better estimates have been obtained by the present authors using only C^0- continuous element (Bleyer and de Buhan, 2013a), dissipation being produced by curvature as well as angular rotation discontinuities. The aim of this work is, thus, to perform yield design computations of plate structures by adapting these numerical methods to the case of complex anisotropic strength criteria computed from homogenization. It will be shown that the yield line method can easily be extended to these criteria without much difficulties, whereas a specific approximation procedure will be required for a complete finite element upper bound approach. It should be noticed that the proposed methods aim at taking advantage of the efficiency of SOCP solvers, which enable to manipulate nonlinear strength criteria, so that a more efficient approximation procedure than piecewise linearization is possible.

Section 2 will first be devoted to the extension of the yield line method to complex strength criteria and an analytical example on a simply supported rectangular plate made of a reinforced material will be presented. Section 3 will present a procedure to approximate a numerically computed three-dimensional yield surface by a convex hull of ellipsoids so that a finite element kinematic approach can be formulated and treated by SOCP solvers. Finally, numerical examples making use of some macroscopic strength criteria previously computed in Part I (Bleyer and de Buhan, 2014) will be investigated.

2. A first attempt at evaluating the bearing capacity of heterogeneous thin plates by the yield line method

2.1. Yield line method for a numerically computed strength criterion

The yield line method is a simple upper bound approach for the yield design of plates in bending which considers only rigid mechanisms separated by yield lines, where jumps of angular velocity have to be taken into account in the expression of the maximum resisting work. The formulation of the corresponding upper bound yield design problem reads as:

$$\underline{Q} \in \Lambda \Rightarrow \forall \widehat{u}\text{K.A. with } \underline{q}, \quad P_{ext}(\widehat{u}) \leqslant P_{rm}(\widehat{u})$$

where $P_{ext}(\widehat{u})$ is the work of external loads in the kinematically admissible velocity field $\widehat{u}$ and

$$P_{rm}(\widehat{u}) = \int_{\Gamma} \Pi([\![\theta_n]\!];\underline{n})dl$$

is the maximum resisting work associated with a set of yield lines Γ of unit normal $\underline{n}$ and angular velocity jumps $[\![\theta_n]\!]$ across Γ following the normal $\underline{n}$. Hence, $\Pi([\![\theta_n]\!];\underline{n})$, which corresponds to a particular value of the support function of the strength criterion associated with rotation discontinuities, is defined as:

$$\Pi([\![\theta_n]\!];\underline{n}) = \sup_{\underline{\underline{M}} \in G} M_{nn}[\![\theta_n]\!] = \Pi(\underline{\underline{\chi}} = [\![\theta_n]\!]\underline{n} \otimes \underline{n})$$

We now consider that the local strength criterion of the plate is a macroscopic strength criterion G^{hom} obtained from a homogenization procedure, as described in the first part of this work. In particular, it is described by its support function $\Pi_{hom}(\underline{\underline{\chi}})$. Using the previous remarks, we have:

$$\Pi([\![\theta_n]\!];\underline{n}) = \Pi_{hom}([\![\theta_n]\!]\underline{n} \otimes \underline{n}) = |[\![\theta_n]\!]|\Pi_{hom}(\underline{n} \otimes \underline{n})$$

since support functions are positively 1-homogeneous. Let $(\underline{e}_x, \underline{e}_y)$ be the orthonormal frame attached to the periodic unit cell, then,

$$\begin{aligned}\Pi([\![\theta_n]\!];\underline{n}) = |[\![\theta_n]\!]|\Pi_{hom}(&\cos^2\alpha(\underline{e}_x \otimes \underline{e}_x) + \sin^2\alpha(\underline{e}_y \otimes \underline{e}_y) \\ &+ \sin 2\alpha(\underline{e}_x \overset{s}{\otimes} \underline{e}_y)) = |[\![\theta_n]\!]|\Pi_0(\alpha)\end{aligned}$$

where α is such that $\underline{n} = \cos\alpha\underline{e}_x + \sin\alpha\underline{e}_y$. Therefore, the support function of rotation discontinuities is entirely described by function $\Pi_0(\alpha)$ depending on the sole normal orientation angle α. This function can be determined by solving a series of auxiliary yield design problems attached to the unit cell with a macroscopic curvature of the form: $\chi_{xx} = \cos^2\alpha$, $\chi_{yy} = \sin^2\alpha$ and $\chi_{xy} = \sin 2\alpha/2$ for different values of α. Fig. 1 represents such a function $\Pi_0(\alpha)$ corresponding to the reinforced plate example presented in the first part of this work is represented. The dependance of this function with respect to α is characteristic of the reinforced plate anisotropy.

Finally, once the geometry of the yield line mechanism has been fixed, $\Pi_0(\alpha)$ can be computed for all yield line normal orientations

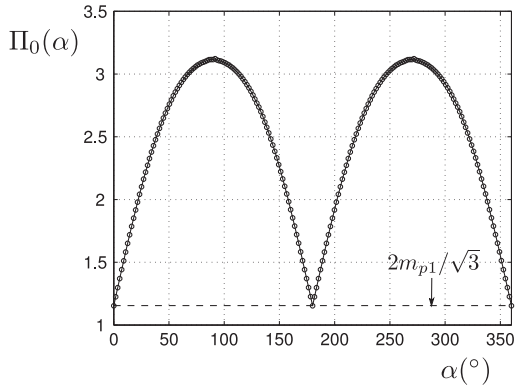

Fig. 1. Function $\Pi_0(\alpha)$ for the reinforced plate example (Bleyer and de Buhan, 2014). The circles correspond to numerically computed values obtained from the resolution of auxiliary yield design problems on the unit cell. The horizontal dotted line corresponds to the value of $\Pi_0(\alpha)$ in the case of an unreinforced von Mises plate with ultimate bending moment $m_{p1} = 1$.

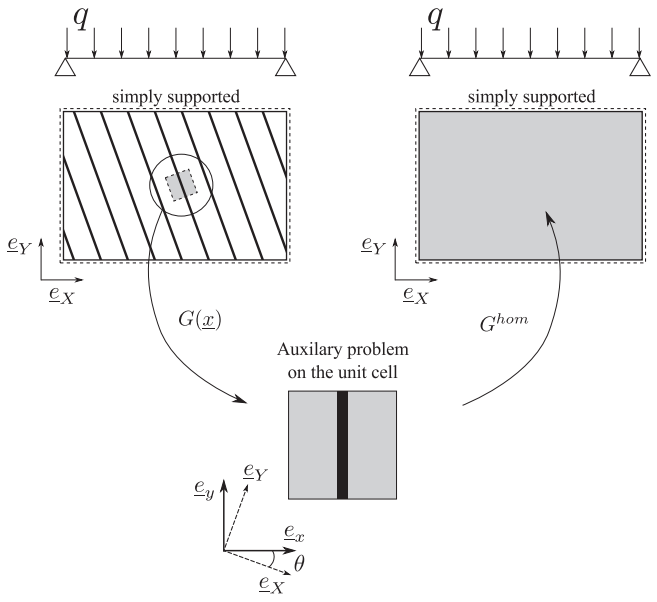

Fig. 2. Homogenization procedure for a rectangular reinforced plate under uniform loading.

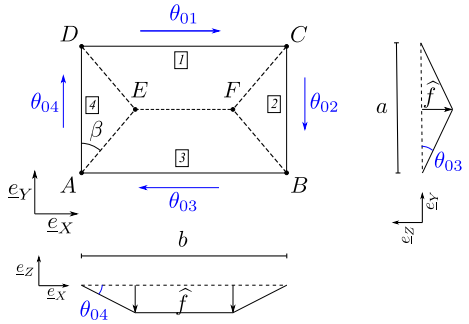

Fig. 3. Mechanism 1 for the rectangular plate under uniform loading.

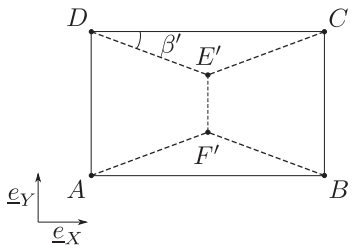

Fig. 4. Mechanism 2 for the rectangular plate under uniform loading.

α by interpolating the numerically computed discrete values, deduced from the auxiliary problem.

2.2. Application to a reinforced rectangular plate under uniform loading

Consider a rectangular plate of length b in the $\underline{e}_X$ direction and a in the $\underline{e}_Y$ direction. The plate strength criterion corresponds to the macroscopic criterion G^{hom} of the reinforced plate example considered in Part I. The reinforcements, oriented along the unit cell direction $\underline{e}_y$, form an angle θ with the $\underline{e}_Y$ direction of the plate (see Fig. 2). The plate is simply supported and loaded by a uniform transversal load $-q\underline{e}_Z$. The objective of this subsection is to determine an upper bound of the ultimate load q^* of such a reinforced plate by considering two different simple yield line mechanisms. For more details on the yield line method, the reader may refer to Save et al. (1997).

2.2.1. Mechanism 1

The first mechanism (Fig. 3) consists of two triangles *BFC* and *AED* (numbered 2 and 4, respectively) parametrized by the same angle β and two trapezes *CDEF* and *ABFE* (numbered 1 and 3). The central yield line *EF* is animated by a uniform vertical velocity $-\widehat{f}\underline{e}_Z$ with $\widehat{f} > 0$. The following upper bound estimate is obtained for the reinforced plate limit load (cf. A):

$$q^* \leqslant q_1 = \min_{\beta \in [0;\arctan(b/a)]} \frac{\frac{4}{\sin 2\beta}(\Pi_0(\beta-\theta)+\Pi_0(\pi-\beta-\theta))+4(b/a-\tan\beta)\Pi_0(\pi/2-\theta)}{ab\left(\frac{1}{2}-\frac{a}{6b}\tan\beta\right)}$$

2.2.2. Mechanism 2

The second mechanism (Fig. 4) is similar to the first one, but with the triangles along the plate length and the trapezes along its width. The expression of the upper bound is very similar to the expression obtained for the first mechanism if one exchanges the role of a and b and replaces β by $\pi/2-\beta'$ (with a special care for the contribution of the yield line $E'F'$ in the expression of P_{rm}). The following upper bound is then obtained:

$$q^* \leqslant q_2 = \min_{\beta' \in [0;\arctan(a/b)]} \frac{\frac{4}{\sin 2\beta'}(\Pi_0(\pi/2-\beta'-\theta)+\Pi_0(\pi/2+\beta'-\theta))+4(a/b-\tan\beta')\Pi_0(\pi-\theta)}{ab\left(\frac{1}{2}-\frac{b}{6a}\tan\beta'\right)}$$

The best upper bound is given by the minimum of q_1 and q_2:

$$q^* \leqslant q_u = \min(q_1, q_2)$$

Both minimization problems are numerically solved for different values of the reinforcement orientation θ for a square plate $a=b=1$ as well as for a rectangular plate with $a=1$ and $b=1.5$. The obtained upper bounds are normalized by a numerical estimate of the corresponding unreinforced plate problem limit load, namely $q_0 = 25.02$ for the square plate and $q_0 = 17.69$ for the rectangular plate.

Results for the reinforced square plate are presented in Fig. 5. These results clearly illustrate the anisotropy effect on the ultimate load, induced by the privileged direction of the reinforcement. Contrary to a isotropic homogeneous square plate for which the optimal mechanism correspond to yield lines along both diagonals,

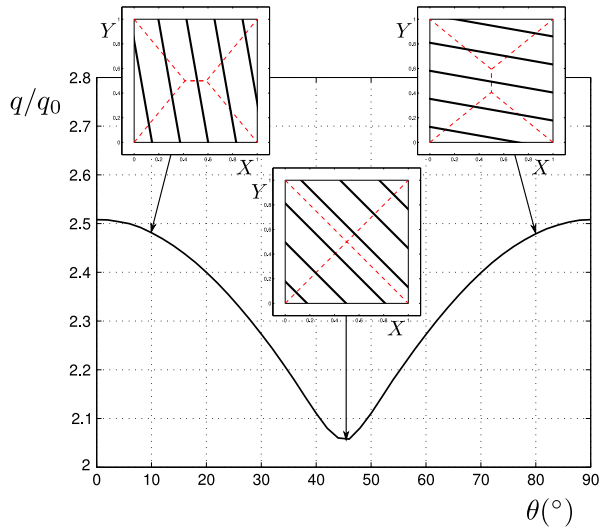

Fig. 5. Yield line upper bound for the reinforced square plate as a function of the reinforcement orientation θ. Optimal yield line mechanisms are represented for $\theta = 10^\circ, \theta = 45^\circ$ and $\theta = 80^\circ$.

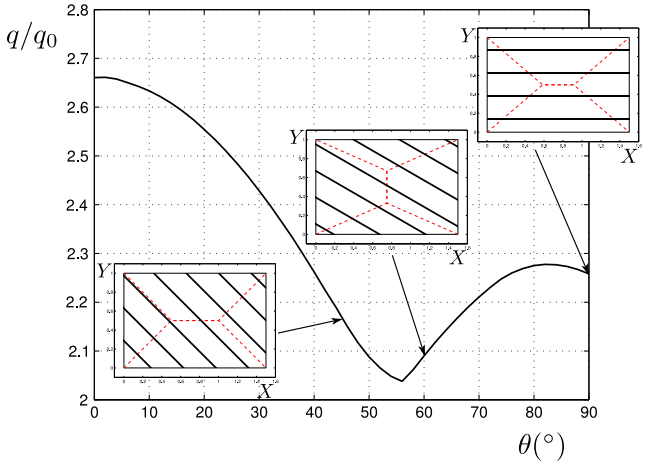

Fig. 6. Yield line upper bound for the reinforced rectangular plate as a function of the reinforcement orientation θ. Optimal yield line mechanisms are represented for $\theta = 45^\circ, \theta = 60^\circ$ and $\theta = 90^\circ$.

optimal yield line layouts and associated upper bound estimates vary with respect to the orientation angle. For instance, the upper bound estimate between the case $\theta = 0^\circ$ and $\theta = 45^\circ$ is decreased by 18%. It is also to be noted that, for angles comprised in the range $0^\circ \leqslant \theta \leqslant 45^\circ$, optimal mechanisms are of type 1, whereas for $45^\circ \leqslant \theta \leqslant 90^\circ$, optimal mechanisms are of type 2, such that the curve of ultimate load estimates is symmetric with respect to $\theta = 45^\circ$.

As regards the rectangular plate problem (Fig. 6), the anisotropy effect is still more pronounced, since the upper bound estimate is decreased by 31% between $\theta = 0^\circ$ and $\theta = 56^\circ$ for which the reinforcement orientation yields the minimum limit load estimate. On this example, the competition between mechanisms 1 and 2 is more complex since optimal mechanisms of type 2 are obtained for values in the range $56^\circ \leqslant \theta \leqslant 74^\circ$.

2.3. Finite element formulation of the yield line method

Yield line method for complex strength criteria can be also easily implemented in a finite element framework. Consider, indeed, a triangular mesh and a linear interpolation of the velocity in each element. These elements are pure yield line elements since dissipation can be only produced by rotation discontinuities through element edges. Let $\{U\}$ denote the global vector of nodal velocities and $\{F\}$ the global loading vector. The normalization of the work of external loads reads as: $P_{ext}(U) = \langle F\rangle\{U\} = 1$. Let N_D denote the number of active edges i.e., all external and internal edges except free edges and simply supported edges (which do not contribute to the maximum resisting work). For a given active edge j, its length l_j and its normal of orientation angle α_j are computed. The value $\Pi_{0j} = \Pi_0(\alpha_j)$ is computed for all edges and the rotation discontinuity is given by $[\![\theta_{nj}]\!] = \langle \Delta\Theta_j\rangle\{U\}$ such that the maximum resisting work is given by:

$$P_{rm}(U) = \sum_{j=1}^{N_D} l_j \Pi_{0j} |\langle \Delta\Theta_j\rangle\{U\}|$$

Finally, the associated linear programming problem reads as:

$$\begin{aligned} q_{YL} = \min_{U,t_j} & \sum_{j=1}^{N_D} l_j \Pi_{0j} t_j \\ \text{s.t.} \quad & \langle F\rangle\{U\} = 1 \\ & |\langle \Delta\Theta_j\rangle\{U\}| \leqslant t_j \quad j = 1,\ldots,N_D \end{aligned} \tag{1}$$

Although the yield line approach may be very attractive due to its simplicity of implementation, it suffers from many drawbacks. The first one is that it is highly dependent on the mesh orientation because rotation discontinuities can occur along the element edges only. Limit load upper bounds produced by a pure yield line finite element computation can be, therefore, highly dependent on the mesh orientation. Different approaches have been proposed in the literature to overcome this drawback (Johnson, 1994; Jennings, 1996; Askes et al., 1999).

Unfortunately, it has been pointed out by Braestrup (1971) that, even if exact solutions can be obtained for some problems, yield line theory fails, in general, to predict the exact limit load even when assuming a very complex mechanism or with an infinitely refined mesh. Indeed, for the simply supported square plate under uniform pressure with a von Mises strength criterion, the yield line theory cannot do better than predict an upper bound which is 10% higher than the exact limit load. This is due to the fact that the exact solution exhibits areas where dissipation is produced by curvature instead of rotation discontinuities only.

3. Upper bound yield design approach with a complex strength criterion

3.1. Numerical challenges

In the previous section, it has been highlighted that the yield line method can be easily extended to the case when the plate strength criterion is complex, provided that function $\Pi_0(\alpha)$ can be computed for all potential yield lines orientations. However, dissipation through curvature has also to be taken into account to obtain better upper bound estimates. Even if a preferred orientation for the rotation discontinuities will still be present due to the fixed positions of the finite element edges, it will be compensated by a localized zone of curvature field so that a finite element approach combining curvature and rotation discontinuities, besides being much more accurate, is also much less sensitive to the mesh layout than a pure yield line approach.

Unfortunately, the yield design problem may become very difficult when dealing with strength criteria of general shape such as those obtained from a homogenization procedure. For example, if the numerical value of the support function is known only on a finite set of curvature directions, the maximum resisting power cannot be analytically expressed in terms of the unknowns of the

problem. The main challenge is, thus, to obtain easy to handle semi-analytical expressions for the support function, tractable by a numerical solver.

Piecewise linear approximation of the strength criterion is one possible approach. Although it was mainly used to approximate classical non-linear strength criterion in the early developments of numerical yield design, one can imagine using this technique to approximate a complex strength criterion obtained from a homogenization procedure and solve the associated linear programming (LP) problem. However, the number of planes required to approximate the strength criterion with a sufficient accuracy may become rapidly large.

The approximation procedure proposed in this work is a further step in this direction, which combines two important ingredients: first, a natural idea is to use primitives of higher order than planes so that a smaller number of these will be required in the approximation process; the second ingredient is to obtain an approximate criterion which can be expressed using conic constraints, in order to take maximum advantage of the efficiency of SOCP optimization solvers.

Based on these two arguments, our goal is to approximate a convex strength criterion using a convex hull of ellipsoids, since the support function of an ellipsoid $\mathcal{E}_i$ can, indeed, be written as:

$$\pi_{\mathcal{E}_i}(\chi) = \|J_i \cdot \chi\| + \mu_i \cdot \chi$$

where $\chi = \{\chi_{xx}\, \chi_{yy}\, 2\chi_{xy}\}^T$, J_i is a 3×3 positive semi-definite upper triangular matrix (defined by the ellipsoid axes length and orientation) and μ_i is the coordinate vector of the ellipsoid center.

It is to be recalled that the support function of the convex hull of two sets A and B is equal to the maximum between the support function of A and that of B. Hence, the support function of the convex hull $CH(\mathcal{E}_i)$ of r ellipsoids $\mathcal{E}_i$ for $i = 1, \ldots, r$ parametrized by J_i and μ_i is given by:

$$\pi_{CH(\mathcal{E}_i)}(\chi) = \max_{i=1,\ldots,r} \{\|J_i \cdot \chi\| + \mu_i \cdot \chi\}$$

which shows that the support function of the convex hull of r ellipsoids can be easily expressed by means of conic constraints.

3.2. Approximation procedure of the strength criterion

In a recent work, the authors proposed a relatively simple algorithm to approximate numerically computed strength criteria using a convex hull of ellipsoids. The general principle of the algorithm will be briefly recalled here, more details may be found in Bleyer and de Buhan (2013b).

Assuming that the support function of the strength criterion is known for M directions, uniformly distributed on the unit sphere in the space of curvature, the following iterative algorithm constructs, at each iteration, an ellipsoid which is a local approximation of the original convex set.

1. Let χ_0 be the direction whose tangent plane is the furthest away from the current approximation $G_{app,r}$;
2. a second-order Taylor expansion of $\Pi(\chi)$ is performed around χ_0;
3. the local radii of curvature of G at χ_0 are computed from the Taylor expansion;
4. a series of ellipsoid with the same curvature and tangent to G at χ_0 are considered;
5. the best ellipsoid is the one which minimizes the root mean squared error between the support function of G and the one of the ellipsoid in the region around χ_0;
6. the optimal ellipsoid $\mathcal{E}_n$ is added to the convex hull of the current approximation $G_{app,r+1} = CU(G_{app,r}, \mathcal{E}_r)$;
7. go to step 1.

This approximation procedure has been applied to the macroscopic strength criterion of the reinforced plate problem. In Fig. 7, the original strength criterion and approximate strength criteria obtained with different number of ellipsoids are represented to assess the performance of the proposed procedure. More precisely, Fig. 8 represents the evolution of the root mean square (RMS) and maximal error made by the approximation procedure as a function of the number r of ellipsoids. It can be observed that the error is rapidly decreasing. Maximum error is of 17% for 10 ellipsoids, 5% for 30 ellipsoids and 2.8% for 50 ellipsoids. The determination of the 50 optimal ellipsoids took less than 2 min.

Finally, it is worth noting that, although inner approximations are initially produced by the algorithm, it is always possible to expand them by an appropriate scaling factor so as to obtain outer approximations of the initial convex set. This was done for the approximating criterion involving 50 ellipsoids.

3.3. Finite element and SOCP formulation

In this subsection, the discrete upper bound kinematic approach on a plate structure, the strength criterion of which has been previously approximated by a convex hull of r ellipsoids, will be presented. The plate is discretized into N_E cubic Hermite triangles (H3) which were introduced in Bleyer and de Buhan (2013a) and successfully used to solve the kinematic approach of the auxiliary problem in Part I.

The curvature at a given Gauss point g in a given element e can be expressed as $\{\chi\} = [B_{e,g}]\{U\}$. The support function at this point is then:

$$\pi^{e,g}_{CH(\mathcal{E}_i)} = \max_{i=1,\ldots,r} \{\|[J_i][B_{e,g}]\{U\}\| + \langle \mu_i \rangle [B_{e,g}]\{U\}\}$$

The contribution of the curvature term to the maximum resisting work is then obtained after integration over all Gauss points of the structure:

$$P^{curv}_{rm} = \sum_{e=1}^{N_E} \sum_{g=1}^{n} c_{e,g} \max_{i=1,\ldots,r} \{\|[J_i][B_{e,g}]\{U\}\| + \langle \mu_i \rangle [B_{e,g}]\{U\}\}$$

where $c_{e,g}$ are constant terms coming from the n-Gauss points quadrature.

As regards the contribution of inter-element rotation discontinuities to the maximum resisting work, the quantities Π_{0j} are directly evaluated as a function of the approximating ellipsoids parameters. Indeed, introducing $\chi_{disc,j} = \{\cos^2 \alpha_j \ \sin^2 \alpha_j \ \sin 2\alpha_j\}^T$:

$$\Pi_{0j} = \pi_{CH(\mathcal{E}_i)}(\chi_{disc,j}) = \max_{i=1,\ldots,r} \left\{\|J_i \cdot \chi_{disc,j}\| + \mu_i \cdot \chi_{disc,j}\right\}$$

so that

$$P^{disc}_{rm} = \sum_{j=1}^{N_D} \Pi_{0j} \sum_{g'=1}^{m} c'_{j,g'} \left|\langle \Delta\Theta_j \rangle \{U\}\right|$$

where $c'_{j,g'}$ are constant terms coming from the m-Gauss points quadrature on edges.

Finally, introducing different auxiliary variables, the upper bound kinematic problem can be formulated as:

$$\begin{aligned} q_u = \min \quad & \sum_{k=1}^{N_E \cdot n} c_k t_{k,0} + \sum_{k'=1}^{N_D \cdot m} \Pi_{0j} c'_{k'} s_{k'} \\ \text{s.t.} \quad & \langle F \rangle \{U\} = 1 \\ & \{r_{k,i}\} = [J_i][B_{e,g}]\{U\} \\ & t_{k,i} \geqslant \|\{r_{k,i}\}\| \qquad i = 1, \ldots, r \\ & t_{k,i} + \langle \mu_i \rangle [B_{e,g}]\{U\} \leqslant t_{k,0} \qquad k = 1, \ldots, n \cdot N_E \\ & u_{k'} = \langle \Delta\Theta_j \rangle \{U\} \\ & s_{k'} \geqslant |u_{k'}| \qquad k' = 1, \ldots, m \cdot N_D \end{aligned} \tag{2}$$

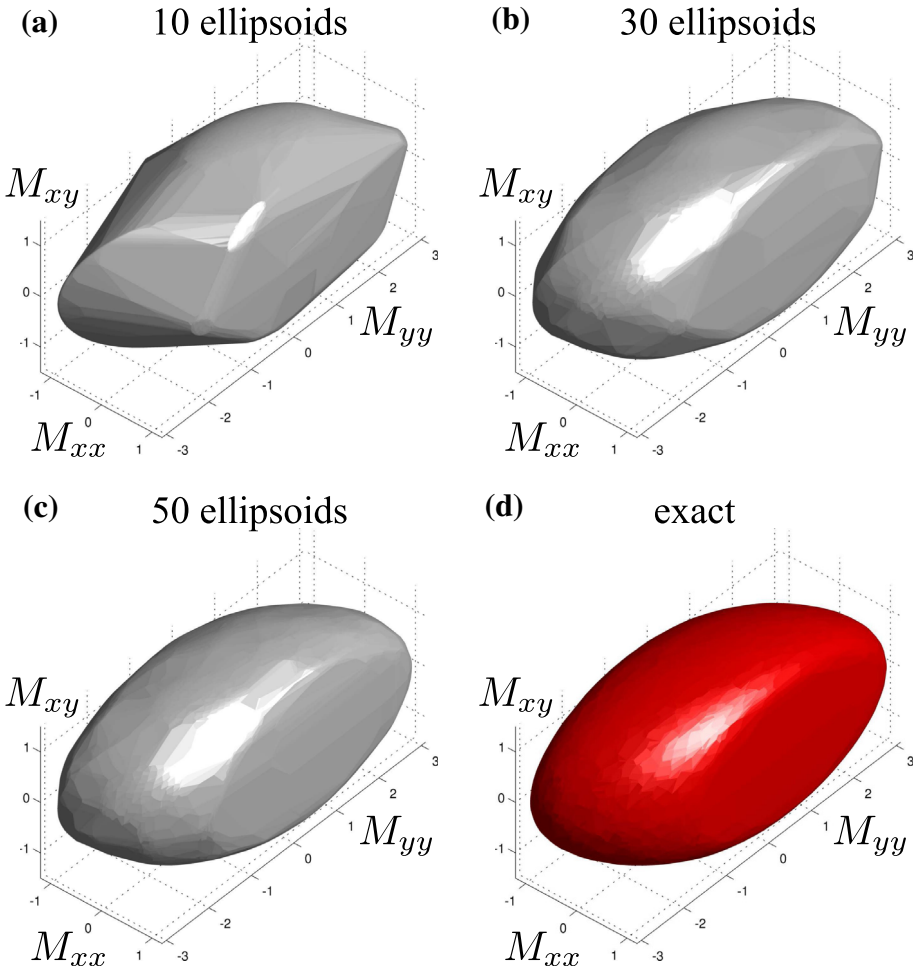

Fig. 7. Approximation procedure of the macroscopic strength domain G^{hom} for the reinforced plate.

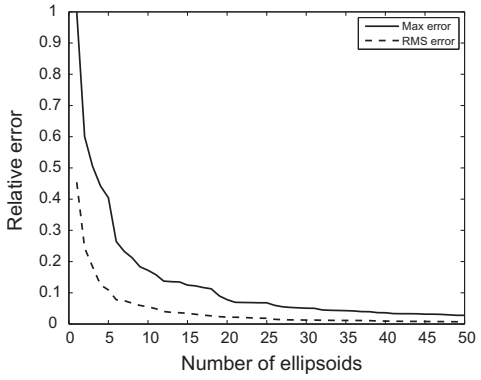

Fig. 8. Evolution of the relative error with the number of ellipsoids. Errors are computed by considering the difference between both support functions.

which is a standard SOCP problem involving $r \cdot n \cdot N_E$ conic constraints, $r \cdot n \cdot N_E + m \cdot N_D$ linear inequality constraints and $1 + 3r \cdot n \cdot N_E + m \cdot N_D$ equality constraints. It is worth noting that, even with a relatively simple mesh of $N_E = 500$ elements, a $n = 3$ Gauss points rule and $r = 50$ ellipsoids, $r \cdot n \cdot N_E = 75,000$ so that (2) already constitutes a large scale SOCP problem.

4. Numerical examples

In this section, numerical examples are presented to assess the performance of the different proposed methods.

In the first example, problem (2) associated to the reinforced plate problem is solved using the MOSEK software package and the influence of the number r of approximating ellipsoids is investigated. The value of r is, indeed, the main factor which determines the difficulty of the optimization problem. It is to be noted that approximations with $r = 10$ and $r = 30$ are not outer approximations of the macroscopic criterion G^{hom} so that a global computation with such domains will not produce an upper bound of the limit load. Therefore, problem (2) has been solved for these values of r, then, in a second step, the so-obtained optimal velocity field $\{U\}$ has been used to evaluate the maximum resisting work with $r = 50$ ellipsoids, the convex hull of which has been considered to be sufficiently close to the original strength criterion. Such a post-processing procedure has been applied to all SOCP upper bounds presented in this section. The numerical yield line problem (1) has also been solved using MOSEK for the reinforced plate problem.

The second example will treat the case of a perforated circular plate and compare the influence of the hole sizes and shapes on the limit load.

4.1. Reinforced plate under uniform loading

Finite element meshes used for the SOCP computations are represented in Fig. 9(a) for the square plate problem and in Fig. 9(b) for the rectangular plate problem. As regards numerical yield line computations, the same type of structured mesh has been used

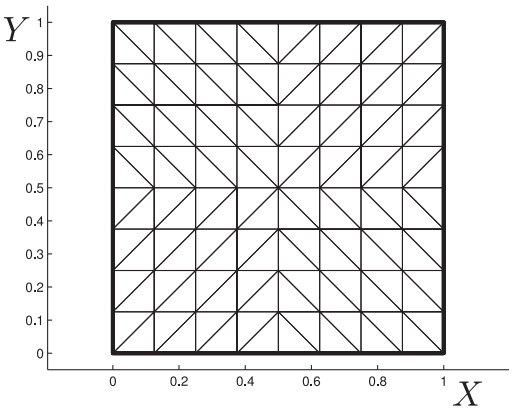

(a) 128 elements mesh for the square plate problem

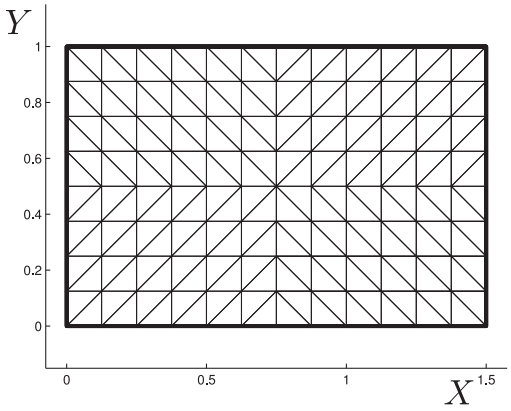

(b) 192 elements mesh for the rectangular plate problem

Fig. 9. Finite element meshes for SOCP computations.

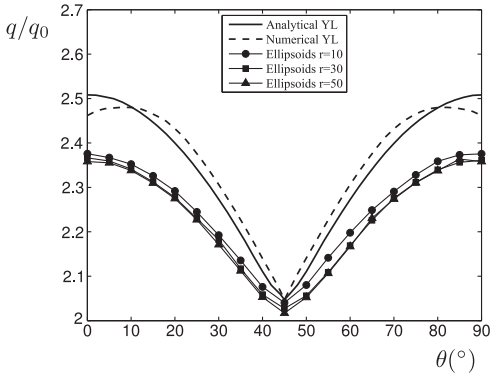

Fig. 10. Comparison of the upper bound estimates for the reinforced rectangular plate obtained with various methods: analytical yield line (YL) method, numerical yield line method, SOCP with a convex hull of $r = 10, 30$ and 50 ellipsoids.

with 1568 elements for the square plate and 3248 elements for the rectangular plate.

In Fig. 10 for the square plate and in Fig. 11 for the rectangular plate, the SOCP upper bounds obtained with $r = 10, 30$ and $r = 50$ ellipsoids have been compared to the upper bound obtained with

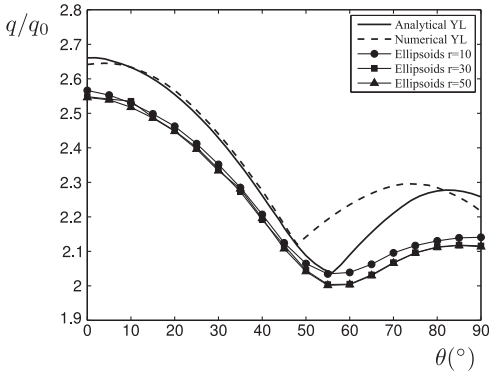

Fig. 11. Comparison of the upper bound estimates for the reinforced rectangular plate obtained with various methods: analytical yield line (YL) method, numerical yield line method, SOCP with a convex hull of $r = 10, 30$ and 50 ellipsoids.

Table 1
Typical optimization times for the SOCP problems on the square and rectangular plate problem. (performed on a Intel-P4 2.4 GHz running Linux 32-bits with Mosek v7.0).

Number of ellipsoids	Square plate (s)	Rectangular plate (s)
$r = 10$	2.5	4
$r = 30$	6.5	13
$r = 50$	12	24

the analytical yield line method of subSection 2.2 as well as to the upper bound obtained with a numerical implementation of the yield line method presented in subSection 2.3. It is first to be noted that numerical yield line upper bound does not necessarily improve the analytical yield line upper bound. This is mainly due to the considered finite element mesh which restrains the potential set of yield lines. In this case too, the numerical yield line method also proved to be highly sensitive to the mesh layout.

Secondly, SOCP computations yield better estimates, by almost 10% in some cases. One can also observe that upper bounds obtained with $r = 30$ or 50 ellipsoids are very close to those obtained with $r = 10$ ellipsoids, differing by less than 2%. Therefore, despite the fact that the original strength criterion is not particularly well approximated with $r = 10$ ellipsoids, it seems that, due to the post-processing procedure, it is sufficient to obtain a good optimal velocity field and related upper bound estimate.

Besides, typical computation times for the optimization procedure have been reported in Table 1. It can be observed that the computational cost on a standard desktop computer is very reasonable even for the highest number of ellipsoids used to describe the yield surface.

Finally, failure mechanisms of the square plate problem have also been represented in Fig. 12 for the homogeneous plate and the reinforced plate with $\theta = 0^\circ$ and $\theta = 45^\circ$. The anisotropy induced by the presence of the reinforcements can be clearly observed for these two cases by comparison to the homogeneous case. For example, with $\theta = 45^\circ$, the optimal mechanism seems exhibit a kind of yield line along the diagonal parallel to the reinforcement direction and a region with a distributed curvature along the other diagonal.

4.2. Perforated circular plate under uniform loading

In this last example, the case of a simply supported circular plate of radius R subject to a uniform loading of intensity q is considered. The plate is made of a von Mises material of ultimate bending moment m_p perforated by a series of circular or square

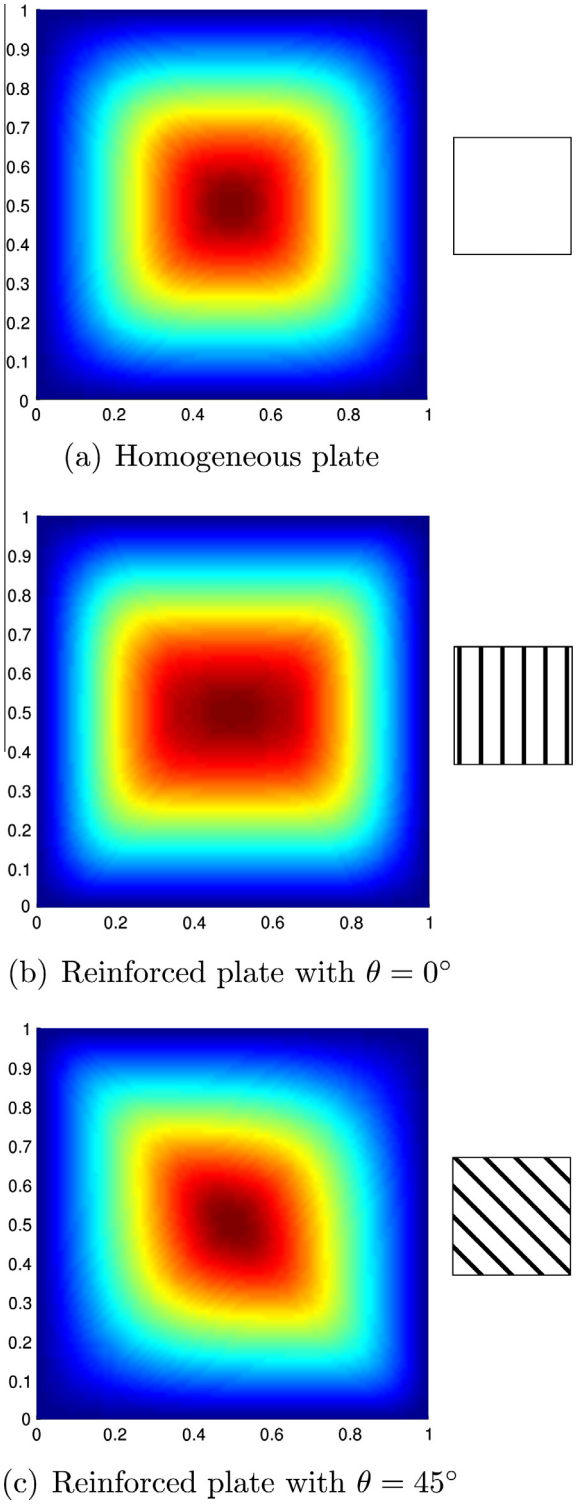

Fig. 12. Comparison of different failure mechanisms for the simply supported square plate.

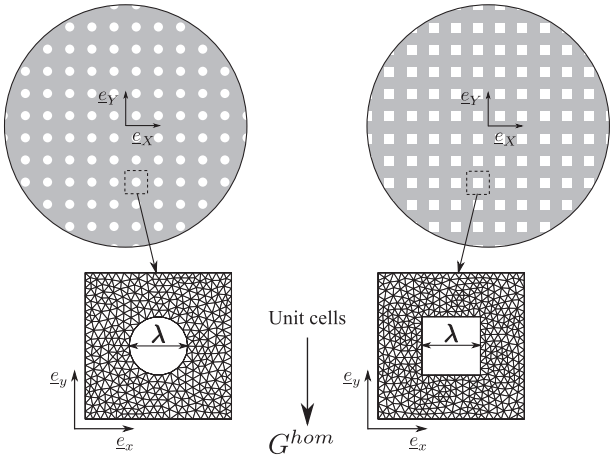

Fig. 13. Circular plate perforated by a series of circular or square holes.

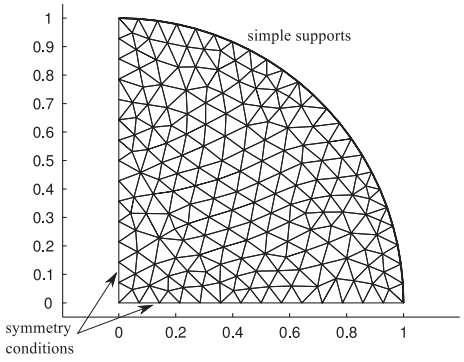

Fig. 14. 413 elements mesh used for the global computation.

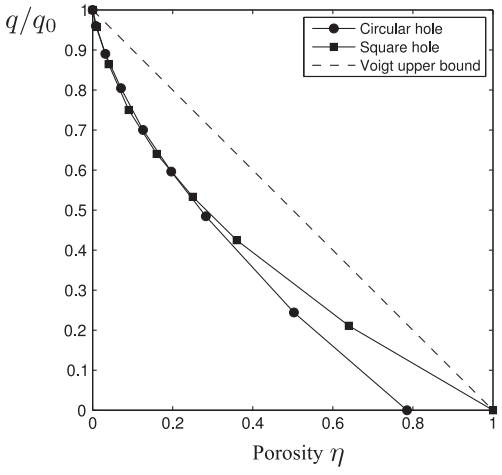

Fig. 15. Evolution of the obtained upper bounds with respect to the plate porosity.

holes arranged as depicted in Fig. 13. Different square unit cells are considered by varying the non-dimensional hole size parameter λ which was respectively taken as $\lambda = 0.1, 0.2, 0.3, 0.4, 0.5, 0.6, 0.8$ for the circular hole as well as for the square hole.

Obviously, for $\lambda = 0$, the solution relative to the homogeneous circular plate problem obeying a von Mises criterion is recovered. For simple supports, the limit load is known to be $q_0 = 6.52 m_p/R^2$ Save et al., 1997. Besides, for $\lambda = 1$, all holes are connected and the plate bearing capacity vanishes which gives then $q = 0$ as the limit load.

The macroscopic strength criterion G^{hom} has been determined by solving the kinematic upper bound auxiliary problem for the 2×7 different unit cell geometries. For one unit cell geometry, 10,000 values of Π_{hom} have been computed in around 1 h. Simultaneous computations have been made to reduce the computational cost. Then, the approximation procedure has been performed to approximate the strength criterion by 50 ellipsoids. This also took

around 2 min for each yield surface. Finally, computations on the homogenized problem have been performed on a quarter of circular plate (see Fig. 14) with 10 ellipsoids and the previously mentioned post-processing step. Each optimization procedure was performed by Mosek in 5–10 s.

In Fig. 15, the ratio between the upper bounds of each homogenized problems and the solution for the homogeneous plate have been represented with respect to the plate porosity defined by $\eta = \pi\lambda^2/4$ in the case of circular holes and $\eta = \lambda^2$ in the case of square holes. The black dotted line represents the Voigt upper bound which is obtained by considering that the exact macroscopic strength criterion is contained in the von Mises criterion with a reduced moment capacity $m_{p,red} = (1-\eta)m_p$, which leads to an upper bound equal to $q_{Voigt} = (1-\eta)q_0$. One can observe that the Voigt upper bound gives a very poor estimate of the limit load for all types of hole shape. Moreover, for a given value in the small porosity range, the limit load does not seem to depend on the hole shape. Finally, considering the evolution of the limit load estimates with respect to the hole size λ, a maximum discrepancy of 6.3% can be observed for $\lambda = 0.5$ between the circular and the square shape.

5. Conclusions and perspectives

In the second part of this work on yield design homogenization method applied to periodic thin plates, the computation of limit load estimates of homogenized plate structure problems derived from upper bound kinematic approaches has been addressed, and associated numerical tools have been proposed. It has been shown, in particular, that the yield line method, which is commonly used in civil engineering computations, can be easily extended to the case of complex strength criteria obtained from homogenization procedures. Indeed, taking advantage of the 1-homogeneity property of support functions and provided that the function $\Pi_0(\alpha)$ depending on the sole normal orientation angle α is determined from the homogenization procedure, the yield line method can be applied, in a straightforward manner, analytically as well as numerically, as shown on the example of the simply supported reinforced rectangular plate.

A more sophisticated and performing upper bound kinematic approach has also been proposed based on the use of finite elements taking into account dissipation through curvature as well as angular jumps. For the curvature term, the support function has no simple expression and an approximation procedure is, thus, required to implement a semi-analytical expression of the support function in the optimization solver. An approximation algorithm based on the construction of a convex hull of ellipsoids is proposed leading to a simple description of the macroscopic strength criterion support function which is compatible with a SOCP formulation. Despite a large number of resulting conic constraints in the global optimization problem, accurate solutions can be obtained in extremely reasonable computing times on a standard desktop. Results indicate that good optimal velocity fields and accurate upper bounds can still be found with a small number (e.g., 10) ellipsoids, a post-processing procedure with a more accurate description of the strength criterion allowing to obtain a more precise upper bound estimate.

Finally, the numerical results indicate that refined kinematic approaches with approximate criteria and SOCP provide better upper bound by at most 15% compared to the yield line method. Therefore, as regards civil engineering applications, the yield line method seems to be a good compromise between implementation simplicity and predictability, although mesh dependency can be an important drawback.

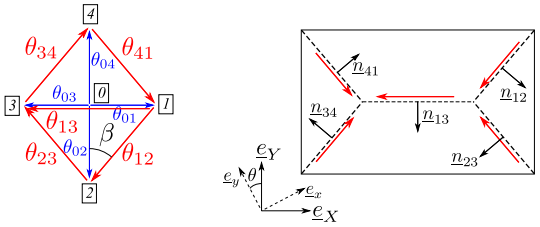

Fig. A.16. Hodograph of angular velocity jumps across yield lines and normal orientations.

Possible extensions of this work are multiple. A first direction of research may consist in applying the general idea of approximating complex strength criteria obtained from homogenization procedures to other mechanical models (plane strain, soils,...). The development of more performing approximation procedures which would require even less primitives to describe the yield surface is also possible. As regards periodic plates, a current work aims at treating the case of the plate thickness being of the same order as the unit cell characteristic length, by solving the auxiliary problems defined on a three-dimensional unit cell with the same numerical tools. Finally, further work can also deal with the case of plates having a finite resistance to shear forces or the more complicated case of shells.

Appendix A. Analytical yield line computations

The work of external loads developed in mechanism 1 is given by:

$$P_{ext}(\widehat{u}) = qab\widehat{f}\left(\frac{1}{2} - \frac{a}{6b}\tan\beta\right)$$

The angular velocity of regions 1 and 3 are given by $\theta_{01} = \theta_{03} = \frac{2\widehat{f}}{a}$, whereas the angular velocity of regions 2 and 4 are given by $\theta_{02} = \theta_{04} = \frac{2\widehat{f}}{a\tan\beta}$. The hodograph of angular velocities represented in Fig. A.16 is used to compute the discontinuity of angular velocity θ_{ij} between regions i and j. We have:

$$\theta_{12} = \theta_{23} = \theta_{34} = \theta_{41} = \frac{2\widehat{f}}{a\sin\beta} \quad \text{and} \quad \theta_{13} = \frac{4\widehat{f}}{a}$$

The orientation angles α_{ij} of the yield line normals $\underline{n}_{ij}$ are given by:

$$\begin{aligned}
\alpha_{12} &= 2\pi - \beta - \theta \\
\alpha_{23} &= \pi + \beta - \theta \\
\alpha_{34} &= \pi - \beta - \theta \\
\alpha_{41} &= \beta - \theta \\
\alpha_{13} &= \pi/2 - \theta
\end{aligned}$$

We also have $|AE| = |BF| = |CF| = |DE| = a/(2\cos\beta)$ and $|EF| = b - a\tan\beta$. Obviously, all expressions are valid only if $\beta \leqslant \arctan(b/a)$. Therefore, the maximum resisting work associated with this mechanism is given by:

$$\begin{aligned}
P_{rm} &= \int_\Gamma |[\![\theta_n]\!]|\Pi_0(\alpha)dl \\
&= 4|CF||\theta_{12}|(\Pi_0(\pi+\beta-\theta)+\Pi_0(\pi-\beta-\theta)+\Pi_0(\beta-\theta)+\Pi_0(\beta-\theta)) \\
&\quad + |EF||\theta_{13}|\Pi_0(\pi/2-\theta)
\end{aligned}$$

Finally, observing that $\Pi_0(\alpha)$ is $\pi-$ periodic and symmetric with respect to $\pi/2$ due to the unit cell symmetry, the following upper bound estimate is obtained for the reinforced plate limit load:

$$q^* \leqslant q_1 = \min_{\beta\in[0;\arctan(b/a)]} \frac{\frac{4}{\sin 2\beta}(\Pi_0(\beta-\theta)+\Pi_0(\pi-\beta-\theta))+4(b/a-\tan\beta)\Pi_0(\pi/2-\theta)}{ab\left(\frac{1}{2}-\frac{a}{6b}\tan\beta\right)}$$

References

Askes, H., Rodrguez-Ferran, A., Huerta, A., 1999. Adaptive analysis of yield line patterns in plates with the arbitrary lagrangian–eulerian method. Comput. Struct. 70, 257–271.

Bleyer, J., de Buhan, P., 2013a. On the performance of non-conforming finite elements for the upper bound limit analysis of plates. Int. J. Numer. Methods Eng. 94, 308–330.

Bleyer, J., de Buhan, P., 2013b. A greedy algorithm for yield surface approximation. C.R. Mec. 341, 605–615.

Bleyer, J., de Buhan, P., 2014. A computational homogenization approach for the yield design of periodic thin plates. Part I: construction of the macroscopic strength criterion. Int. J. Solids Struct. 51, 2448–2459.

Bræstrup, M., 1971. Yield-line theory and limit analysis of plates and slabs, Danmarks Tekniske Højskole, Afdelingen for Bærende Konstruktioner.

Capsoni, A., Corradi, L., 1999. Limit analysis of plates – a finite element formulation. Struct. Eng. Mech. 8, 325–341.

de Buhan, P., 1986. A Fundamental Approach to the Yield Design of Reinforced Soil Structures (Ph.D. thesis). Thèse d'Etat, Paris VI, 1986.

Francescato, P., Pastor, J., 1998. Résistance de plaques multiperforées: comparaison calcul-expérience. Rev. Eur. Élém. Finis 7, 421–437.

Hassen, G., Gueguin, M., de Buhan, P., 2013. A homogenization approach for assessing the yield strength properties of stone column reinforced soils. Eur. J. Mech. A. Solids 37, 266–280.

Jennings, A., 1996. On the identification of yield-line collapse mechanisms. Eng. Struct. 18, 332–337.

Johansen, K., 1962. Yield-line Theory. Cement and Concrete Association, London.

Johnson, D., 1994. Mechanism determination by automated yield-line analysis. Struct. Eng. 72, 323.

Le, C., Nguyen-Xuan, H., Nguyen-Dang, H., 2010. Upper and lower bound limit analysis of plates using FEM and second-order cone programming. Comput. Struct. 88, 65–73.

Maghous, S., 1991. Détermination du critère de résistance macroscopique d'un matériau hétérogène à structure périodique. Approche numérique, These, Ecole Nationale des Ponts et Chaussées.

Maghous, S., de Buhan, P., Bekaert, A., 1998. Failure design of jointed rock structures by means of a homogenization approach. Mech. Cohesive-frictional Mater. 3, 207–228.

Marigo, J.-J., Mialon, P., Michel, J.-C., Suquet, P., 1987. Plasticité et homogénéisation: un exemple de prévision des charges limites d'une structure hétérogène périodique. J. Méc. Théor. Appl. 6, 47–75.

Milani, G., Loureno, P., Tralli, A., 2006. Homogenization approach for the limit analysis of out-of-plane loaded masonry walls. J. Struct. Eng. 132, 1650–1663.

Munro, J., Da Fonseca, A., 1978. Yield line method by finite elements and linear programming. Struct. Eng. 56, 37–44.

Pastor, J., Turgeman, S., 1983. Approche numérique des charges limites pour un matériau orthotrope de révolution en déformation plane. J. Méc. Théor. Appl. 2, 393–416.

Sab, K., 2003. Yield design of thin periodic plates by a homogenization technique and an application to masonry walls. C.R. Mec. 331, 641–646.

Save, M., Massonnet, C., de Saxce, G., 1997. Plastic Limit Analysis of Plates, Shells, and Disks, vol. 43. North Holland.

Suquet, P., 1985. Elements of homogenization for inelastic solid mechanics. Homogenization Tech. Compos. Media 272, 193–278.

Turgeman, S., Pastor, J., 1987. Comparaison des charges limites d'une structure hétérogène et homogénéisée. J. Méc. Théor. Appl. 6, 121–143.